Prediction of water retention properties of French soils using the in situ volumetric water content at field capacity as single input data

Hassan Al Majou, Ary Bruand

Soil & Tillage Research xxx (xxxx) 105750

Contents lists available at ScienceDirect

Soil & Tillage Research

journal homepage: www.elsevier.com/locate/still

Prediction of water retention properties of French soils using the in situ volumetric water content at field capacity as single input data

Hassan Al Majou [a, b], Ary Bruand [a, *]

[a] Université d'Orléans, CNRS, BRGM, Institut des Sciences de la Terre d'Orléans (ISTO), Observatoire des Sciences de l'Univers en région Centre, 1A rue de la Férollerie, 45071 Orléans, France

[b] Université de Damas, Département des Sciences du Sol, Faculté Agronomique, P.O. Box 30621, Damascus, Syria

ARTICLE INFO

Keywords:
Artificial neural network
Coefficient of determination
Pedotransfer functions
Root mean squared error
Simple linear regression
Support vector machines

ABSTRACT

The objective of this study was to investigate the relevance of using the in situ volumetric water content at field capacity (θ_{FC}) as a predictor of the water retention properties by comparing the performances of pedotransfer functions (PTFs) established using artificial neural networks (ANN-PTFs) and support vector machines (SVM-PTFs) with much simpler PTFs in the form of simple linear regressions (SLR-PTFs). A dataset comprising 456 horizons collected in soils located in France was used. The available data were: the silt and clay contents (SC), the organic carbon content (OC), the bulk density at field capacity (BD^m_{FC}), the in situ gravimetric water content at field capacity (W^m_{FC}) related to θ_{FC} by using BD^m_{FC}, and the volumetric water content at –1, –3.3, –10, –33, –100, –330 and –1500 kPa matric potential. The performances of the PTFs studied were compared by using the root mean squared error (RMSE) and the coefficient of determination (R^2). Our results showed the relevance of using θ_{FC}, which was proved to be close to the volumetric water content at –10 kPa matric potential, as a predictor of the water retention properties. With ANN-PTFs, the best performances were recorded when both θ_{FC} and SC were used as input data (RMSE = 0.027 $cm^3\ cm^{-3}$ and R^2 = 0.92). With SVM-PTFs, the smallest RMSE was recorded when θ_{FC} was used as single input data (RMSE = 0.026 $cm^3\ cm^{-3}$). As for R^2 of SVM-PTFs, it was the highest with θ_{FC} and SC as input data (R^2 = 0.84). The SLR-PTFs using θ_{FC}as single predictor after stratification by texture performed better (RMSE = 0.031 $cm^3\ cm^{-3}$ and R^2 = 0.88) than the ANN-PTFs using one or two soil characteristics as input data. Comparison of SLR-PTFs with SVM-PTFs showed that the latter performed slightly better than SLR-PTFs after stratification by texture but R^2 was smaller when $\theta_{FC}$was used as the single predictor. Use of a predicted value of the bulk density at field capacity to obtain a value of in situ volumetric water content at field capacity led to poorer performances of the SLR-PTFs but after stratification by texture they remained close to those recorded with ANN-PTFs or SVM-PTFs when they used a single soil characteristic as input data. Finally, our results showed that associating OC to the input data did not increase the perfomances of the ANN-PTFs and SVM-PTFs.

1. Introduction

Since the early work by Briggs and Lane (1907) and Veihmeyer and Hendrickson (1927), predicting difficult-to-measure soil properties has been the subject of many studies (van Looy et al., 2017). During the 80 s, the concept of transfer function emerged (Bouma and van Lanen, 1987) followed by that of pedotransfer function (PTF) (Bouma, 1989) which is now used worldwide. PTFs translate the soil information we have into soil information we need but do not have (Bouma, 1989). Among the very high number of studies dealing with PTFs, those aiming at predicting the water retention properties of soil using PTFs have been the most numerous in the last four decades (e.g. Rawls et al., 1982; Vereecken et al., 1989; Wösten et al., 1999; Minasny et al., 1999; Bruand et al., 2003; Nemes et al., 2003; Pachepsky et al., 2006; Al Majou et al., 2007, 2008a, 2018, 2021; Babaeian et al., 2015; van Looy et al., 2017; Singh et al., 2020; Zhang et al., 2020; Cueff et al., 2021; Tian et al., 2021). Several reviews of the literature on PTFs to predict the water retention properties of soils were also published within the same period (e.g. Wösten et al., 2001; Baker, 2008; Vereecken et al., 2010; Minasny and Hartemink, 2011; Botula et al., 2014; Patil and Singh, 2016; van Looy et al., 2017).

* Corresponding author.
E-mail address: Ary.Bruand@univ-orleans.fr (A. Bruand).

https://doi.org/10.1016/j.still.2023.105750
Received 16 September 2022; Received in revised form 20 March 2023; Accepted 3 May 2023
0167-1987/

Most studies concerned the mathematical tools and the performance of the predictions recorded rather than the nature of the soil characteristics used to establish PTFs. Since the early studies, information about the soil used by PTFs consisted mainly of particle size distribution, bulk density and organic carbon content (e.g. Petersen et al., 1968; Reeve et al., 1973; Gupta and Larson, 1979; Rawls et al., 1982; De Jong and Loebel, 1982; Williams et al., 1983; Pachepsky and Rawls, 1999; Cornelis et al., 2001), with some studies combining the latter with the volumetric water content at –33 and –1500 kPa matric potential (e.g. Rawls et al., 1982, Schaap et al., 1998; 2001; Børgesen and Schaap, 2005; Twarakavi et al., 2009).

PTFs using multilinear regression (MLR) equations were first developed (e.g. Gupta and Larson, 1979; Paydar and Cresswell, 1996; Wösten et al., 2001; Vereecken et al., 2010; Ribeiro et al., 2018; Kalumba et al., 2021), followed by PTFs using artificial neural networks (ANNs) which do not require explicit relations between input data (available soil characteristics) and output data (water retention properties needed but not available) (Pachepsky et al., 1996; Shaap and Bouten, 1996; Schaap et al., 1998, 2001; Minasny et al., 1999). It is still a matter of debate, however, whether the prediction performance by PTFs that use ANNs is an improvement over that recorded with MLR equations and other types of PTFs (Koekkoek and Bootlink, 1999; Nemes et al., 2006; Jana et al., 2007; Kværnø and Haugen, 2011; Haghverdi et al., 2012; Khlosi et al., 2016). Support vector machines (SVM), a data mining tool that uses a supervised non-parametric statistical learning method, were developed to establish PTFs these last ten years (van Looy et al., 2017). Some studies showed that SVMs outperformed ANNs (Lamorski et al., 2008; Twarakavi et al., 2009) while more recent studies did not confirm this (Skalova et al., 2011; Haghverdi et al., 2012).

Generally, the data used were restricted to the soil characteristics available in the databases, i.e. consistently with the initial definition of the concept of PTF as defined by Bouma and van Lanen (1987) and Bouma (1989). Thus, during the last three decades, PTFs have used mainly clay, silt and sand contents, bulk density, organic carbon or organic matter content, and secondarily volumetric water content at –33 and –1500 kPa matric potential which are the prevalent soil characteristics in the soil databases (Batjes et al., 2020). As a result, studies aiming at finding soil characteristics that are easily measurable but poorly represented in databases remained limited. Moreover, the question of the prediction performance versus the complexity of the PTFs used or versus the complexity of the statistical tools required to establish and use the PTFs also remains under discussion. A comparison of the performance of PTFs capable of predicting the volumetric water content at particular values of the matric potential (point PTFs) according to PTF characteristics (class-PTFs versus continuous-PTFs, PTFs based on regression techniques versus PTFs based on machine-learning techniques, easily accessible input data versus less easily accessible input data) shows that we cannot conclude clearly on their respective performances (Table 1).

In that context, the objective of the present study was therefore to compare the performance of PTFs established using machine-learning techniques (ANN or SVM), which can be considered as among the most effective PTFs, with the performance recorded for much simpler PTFs that use only the easily measurable in situ volumetric water content at field capacity, i.e. after excess water contained in macropores has drained away by gravity action in the field (Reeve et al., 1977; Twarakavi et al., 2009a, 2009b). We show that water retention properties, which remain unmeasurable by most soil users, can be predicted with a precision similar to that recorded with machine-learning techniques by using regression techniques and the in situ volumetric water content at field capacity, without or after stratification by texture.

2. Materials and methods

2.1. The soils studied

The study was conducted using a set of 456 horizons comprising 139 topsoil (from 0 to 30 cm depth) and 317 subsoil horizons (> 30 cm depth) collected in Cambisols, Luvisols, Albelivisols, Podzols, and Fluvisols (IUSS Working Group WRB, 2015) located mainly in the Paris Basin, and secondarily in the Pyrenean piedmont plain and western coastal marshlands (Al Majou et al., 2008a, 2008b).

A set of 91 horizons comprising 28 topsoil and 63 subsoil horizons was randomly constituted to test the PTFs (test dataset), while the remaining 365 horizons, comprising 111 topsoil and 254 subsoil horizons, were used to establish the PTFs (training dataset) (Table 2). The soils were sampled in winter when the soil was at field capacity (Bruand et al., 1994, 1996, 2004). The particle size distribution (sand content, Sa, silt content, Si, and clay content, Cl) was measured using the pipette method after pre-treatment with hydrogen peroxide and sodium hexametaphosphate (Robert and Tessier, 1974). The organic carbon content (OC, g kg^{-1}) was measured by oxidation using excess potassium dichromate in sulphuric acid at 135 °C (Baize, 2000), and cation exchange capacity (CEC, $cmol_c$ kg^{-1} of oven-dried soil) using the cobalt-hexamine trichloride method (Ciesielski and Sterckeman, 1997). The bulk density (BD^m_{FC}, g cm^{-3}) was measured with cylinders 1236 cm^3 in volume taken when the soil was at field capacity which corresponds to the water content after evacuation of the excess water contained in macropores by gravity (Reeve et al., 1977; Twarakavi et al., 2009a, 2009b). This corresponds to about 3 days for coarse textured soils and to 5 days for medium to fine textured soils after a period of rain or irrigation long enough to saturate or to nearly saturate the soil porosity by water (Twarakavi et al., 2009a, 2009b). The gravimetric water content of the soil in the cylinder was determined and then considered as the in situ gravimetric water content at field capacity (W^m_{FC}, g g^{-1}). The gravimetric water content at different water potentials was determined by using a pressure membrane or plate apparatus, depending on the pressure applied (Bruand et al., 1996, 2004) for the 456 horizons data set at –1 (W^m_1), –3.3 ($W^m_{3.3}$), –10 (W^m_{10}), –33 (W^m_{33}), –100 (W^m_{100}), –330 (W^m_{330}) and –1500 kPa (W^m_{1500}) water matric potential by using undisturbed samples (10–15 cm^3) collected when the soil was at field capacity (Bruand et al., 1994, 1996; Bruand and Tessier, 2000). The volumetric water content for each horizon at field capacity (θ_{FC}, cm^3 cm^{-3}) and each water matric potential (θ^m_1, $\theta^m_{3.3}$, θ^m_{10}, θ^m_{33}, θ^m_{100}, θ^m_{330} and θ^m_{1500}, cm^3 cm^{-3}) was computed using the BD^m_{FC} of the horizon.

2.2. The soil water retention pedotransfer functions used

2.2.1. Pedotransfer function based on artificial neural networks

The structure of PTFs based on artificial neural networks (ANN-PTFs) used here consists of a three-layer feed-forward back-propagation network using, for each model, input layers (basic soil properties), hidden layers and output layers (soil water retention properties). Each neuron of the hidden layer calculates the sum s, of a weighted combination w_i, of its input signals x_i, and a bias term w_0, and passes the result through the activation functions that are tangent hyperbolic and linear in hidden and output layers, respectively. The Levenberg-Marquardt algorithm (Demuth and Beale, 2000) was implemented to speed up the training of the multi-layer feed-forward neural network. The number of neurons in the hidden layer has to be found through trial and error; the number tested here varied from 1 to 10 neurons. The training was stopped whenever the error increased during cross-validation. Back-propagation algorithms aim at minimizing the error (they minimize the sum of squares of the residuals between the measured and predicted outputs) of the mathematical system represented by the neural network's weights. The error is estimated as the difference between the actual and the computed output.

Table 1
Type of predictive model, characteristics of input and output data and performance of a selection of point PTFs used to predict the volumetric water content at different values of matric potential.

Reference	Country	N	Predictive model	Input data	Output data	N'	R^2	RMSE
Pachepsky et al. (1996)	Hungary	230	PR	< 0.002, 0.002–0.005, 0.005–0.01, 0.01–0.02, 0.02–0.05, 0.05–0.25, BD	$\theta_{0.1}$, θ_1, $\theta_{3.2}$, θ_{10}, θ_{20}, θ_{50}, θ_{250}, θ_{1600}	230	0.66 – 0.97	0.012–0.035
			ANN	< 0.002, 0.002–0.005, 0.005–0.01, 0.01–0.02, 0.02–0.05, 0.05–0.25, BD	$\theta_{0.1}$, θ_1, $\theta_{3.2}$, θ_{10}, θ_{20}, θ_{50}, θ_{250}, θ_{1600}	230	0.68 – 0.97	0.013–0.025
Koekkoek and Bootlink (1999)	Great Britain and The Netherlands	343	ANN	Type of horizon (topsoil or subsoil), < 0.002, 0.002–0.050, 0.050–2, BD, OM	θ_0, θ_{10}, θ_{1500}	136	0.80 – 0.93	0.027 – 0.48
Merdun et al. (2006)	Turkey	130	ANN	< 0.002, 0.002–0.050, 0.050–2, BD, OC, P_1^d, P_2^d, P_3^d	θ_{33}, θ_{1500}	65	0.84 – 0.95	0.020 – 0.051
			MLR	< 0.002, 0.002–0.050, 0.050–2, BD, OC, P_1^d, P_2^d, P_3^d	θ_{33}, θ_{1500}	65	0.93 – 0.98	0.013 – 0.037
Al Majou et al. (2008a)	France	456	DC	Texture classes (5)	θ_1, $\theta_{3.3}$, θ_{10}, θ_{33}, θ_{100}, θ_{330}, θ_{1500}	197	-	0.044
				Texture classes (5), BD	θ_1, $\theta_{3.3}$, θ_{10}, θ_{33}, θ_{100}, θ_{330}, θ_{1500}	197	-	0.033
				Texture classes (5), type of horizon (topsoil or subsoil)	θ_1, $\theta_{3.3}$, θ_{10}, θ_{33}, θ_{100}, θ_{330}, θ_{1500}	197	-	0045
				Texture classes (5), BD, type of horizon (topsoil or subsoil)	θ_1, $\theta_{3.3}$, θ_{10}, θ_{33}, θ_{100}, θ_{330}, θ_{1500}	197	-	0.035
Nguyen et al. (2015)	Vietnam	160	SVM	< 0.002, 0.002–0.05, 0.05–2, BD, OC	θ_1, θ_3, θ_6, θ_{10}, θ_{20}, θ_{33}, θ_{100}, θ_{1500}	160	0.78 – 0.83	0.039 – 0.055[c]
			kNN	< 0.002, 0.002–0.05, 0.05–2, BD, OC	θ_1, θ_3, θ_6, θ_{10}, θ_{20}, θ_{33}, θ_{100}, θ_{1500}	159	0.68 – 0.79	0.045 – 0.059[c]
Dobarco et al. (2019)	France	689	DC	Texture classes (5), BD	θ_{10}, θ_{1500}	308	0.38 – 0.52	0.048 – 0.058
			DC	Texture classes (5), type of horizon (topsoil or subsoil), BD	θ_{10}, θ_{1500}	308	0.46 – 0.54	0.047 – 0.054
			MLR	< 0.002, 0.05–2, OC, BD	θ_{10}, θ_{1500}	308	0.69 – 0.83	0.034 – 0.043
			MLR	Type of horizon (topsoil or subsoil), < 0.002, 0.05–2, OC, D_b	θ_{10}, θ_{1500}	308	0.66 – 0.85	0.027 – 0.043
Singh et al. (2020)	International	138	ANN	< 0.002, 0.002–0.05, 0.05–2, BD, OM, pF	$\theta_{0.01}$ – θ_{2000}	35	0.80	0.046
				< 0.002, 0.002–0.05, 0.05–2, pF	$\theta_{0.01}$ – θ_{2000}	35	0.70	0.056
				< 0.002, 0.002–0.05, 0.05–2, BD, pF	$\theta_{0.01}$ – θ_{2000}	35	0.79	0.047
				< 0.002, 0.002–0.05, 0.05–2, OM, pF	$\theta_{0.01}$ – θ_{2000}	35	0.75	0.051
	International and Turkey	173	ANN	< 0.002, 0.002–0.05, 0.05–2, BD, OM, pF	$\theta_{0.01}$ – θ_{2000}	79	0.76	0.061
				< 0.002, 0.002–0.05, 0.05–2, pF	$\theta_{0.01}$ – θ_{2000}	79	0.61	0.081
				< 0.002, 0.002–0.05, 0.05–2, BD, pF	$\theta_{0.01}$ – θ_{2000}	79	0.74	0.064
				< 0.002, 0.002–0.05, 0.05–2, OM, pF	$\theta_{0.01}$ – θ_{2000}	79	0.69	0.092
Kalumba et al. (2021)	Zambia	211	MLR	< 0.002, 0.002–0.05, 0.05–2, BD, OM, N, STON, ELE, EC, pH, Dep	θ_0, θ_1, θ_{10}, θ_{63}, θ_{250}, θ_{1500}	91	0.52 – 0.88[a]	0.020 – 0.040[a]
			ANN	< 0.002, 0.002–0.05, 0.05–2, BD, OM, N, STON, ELE, EC, pH, Dep	θ_0, θ_1, θ_{10}, θ_{63}, θ_{250}, θ_{1500}	91	0.64 – 0.81[a]	0.020 – 0.040[a]
			RF	< 0.002, 0.002–0.05, 0.05–2, BD, OM, N, STON, ELE, EC, pH, Dep	θ_0, θ_1, θ_{10}, θ_{63}, θ_{250}, θ_{1500}	91	0.62 – 0.85[a]	0.030 – 0.050[a]
			SVM	< 0.002, 0.002–0.05, 0.05–2, BD, OM, N, STON, ELE, EC, pH, Dep	θ_0, θ_1, θ_{10}, θ_{63}, θ_{250}, θ_{1500}	91	0.69 – 0.76[a]	0.030 – 0.050[a]
Bagnall et al. (2022)	USA Canada Mexico	1731	MLR	< 0.002, 0.05–2, OC	θ_{33}, θ_{1500}	1797	0.64 – 0.88	0.015 – 0.032
Amorim et al. (2022)	Brazil	24	MLR	< 0.002[b], 0.05–0.5, 0.05–2, OC, MA, MI, TP, BD, Pd	θ_2 – θ_{1500}	30	0.61 – 0.99	0.017 – 0.127

N: number of horizons in the training dataset; N': number of horizons in the test dataset;
R: coefficient of determination; ME: mean error in $cm^3\ m^{-3}$; RMSE: root mean squared error in $cm^3\ cm^{-3}$;
DC: direct correspondence between classes of composition and water retention properties (class pedotransfer); MLR: multilinear regression; ANN: artificial neural network; SVM: support vector machine; RF: random forest;
< 0.002: particles smaller than 0.002 mm in diameter; 0.002–0.05: particles ranging from 0.002 to 0.05 mm in diameter; 0.05–2: particles ranging from 0.05 to 2 mm in diameter; Textural classes(n): texture with n texture classes; BD: bulk density; OM: organic matter content, OC: organic carbon content; N: nitrogen content,

STON: stoniness; ELE: topographic elevation; EC: electrical conductivity; Dep: depth of upper and lower boundary; MA: macroporosity; MI: microporosity; TP: total porosity; Pd: particle density; θ_h: volumetric water content at the matric potential h in kPa;
[a]: estimated from the graphs; [b]: water-dispersible clay

Table 2
Descriptive statistics of the main characteristics of the soil data sets used in this study.

	Coarse elements (%)	Particle size distribution (%)			OC g kg^{-1}	$CaCO_3$ g kg^{-1}	CEC cmol$_c$ kg^{-1}	BD^m_{FC} g cm^{-3}	θ_{FC} cm^3 cm^{-3}	Volumetric water content (cm^3 cm^{-3}) measured at matric potential h (θ^m_h) in kPa						
	>2000 µm	<2 µm	2-50 µm	50-2000 µm						θ^m_1	$\theta^m_{3.3}$	θ^m_{10}	θ^m_{33}	θ^m_{100}	θ^m_{330}	θ^m_{1500}
	Total dataset (n = 456)															
mean	<1	29.3	43.8	26.9	6.0	54.2	14.8	1.52	0.316	0.354	0.335	0.315	0.289	0.259	0.221	0.187
s.d.	–	15.4	21.8	25.6	5.1	171.3	9.0	0.15	0.071	0.068	0.070	0.075	0.076	0.079	0.076	0.073
min.	–	1.9	1.6	0.1	0.0	0.0	0.6	0.95	0.091	0.134	0.100	0.080	0.056	0.045	0.033	0.013
max.	–	92.9	82.1	95.4	28.8	982	52.8	1.98	0.566	0.605	0.596	0.586	0.557	0.510	0.462	0.370
	Training datset (n = 365)															
mean	<1	29.6	43.4	27.0	6.1	58.5	14.8	0.15	0.072	0.352	0.333	0.313	0.287	0.260	0.222	0.187
s.d.	–	15.4	21.6	25.8	5.1	182.3	9.0	1.00	0.091	0.069	0.072	0.077	0.077	0.080	0.076	0.074
min.	–	1.9	1.6	0.1	0.0	0.0	0.6	1.98	0.566	0.134	0.100	0.080	0.056	0.045	0.033	0.013
max.	–	92.9	82.1	95.4	28.2	982	52.8	1.53	0.322	0.605	0.596	0.586	0.557	0.510	0.462	0.370
	Test dataset (n = 91)															
mean	<1	28.2	45.6	26.1	5.4	37.0	14.5	0.95	0.135	0.362	0.344	0.323	0.294	0.256	0.220	0.187
s.d.	–	15.6	23.0	24.7	4.9	116.3	9.0	1.84	0.561	0.062	0.064	0.067	0.071	0.078	0.075	0.069
min.	–	3.6	5.4	1.9	0.0	0.0	2.0	1.52	0.316	0.139	0.120	0.097	0.078	0.048	0.035	0.028
max.	–	78.6	80.3	90.0	28.8	523.0	45.9	0.15	0.071	0.565	0.548	0.534	0.494	0.476	0.415	0.370

s.d., min, max are the standard deviation, minimum and maximum of soil variables. OC: organic carbon content; $CaCO_3$: calcium carbonate content; CEC: cation exchange capacity; BD^m_{FC}: bulk density measured at field capacity; θ_{FC}: in situ volumetric water content at field capacity.

The ANNs were performed using the neural network toolbox provided by MATLAB® (ver. R2019b). Cross-validation was performed with 15% of the training dataset (Table 2). The parameters at the end of the training process minimized the root mean squared errors of predictions over all matric potentials. The soil characteristics Si and Cl were used together (referred to as SC in the rest of the text when used together as input data) successively associated with one up to three of the following input data BD^m_{FC}, OCand θ_{FC}. Then, values of volumetric water content at water matric potentials of –1 (θ^p_1), –3.3 ($\theta^p_{3.3}$), –10 (θ^p_{10}), –33 (θ^p_{33}), –100 (θ^p_{100}), –330 (θ^p_{330}) and –1500 kPa (θ^p_{1500}) were predicted for the test dataset (Table 2).

2.2.2. Pedotransfer function based on support vector machine

Pedotransfer functions based on support vector machine (SVM-PTFs), another data mining tool to build PTFs, were also used (Twarakavi et al., 2009a, 2009b; Vapnik, 2013). The principles of support vector machine algorithms can be found in Lamorski et al. (2008), Twarakavi et al. (2009a), (2009b) and van Looy et al. (2017). The support vector machine algorithms were performed using the Deep learning toolbox provided by MATLAB® (ver. R2019b). The designated data to train, cross-validate and test as well as the input and output variables were identical to those used for ANN. The training dataset was used to optimize the SVM model using a grid search alogorithm and a k-fold cross-validation procedure with k = 5 to prevent over-fitting. The SVM parameters at the end of the training process minimized the root mean squared errors of predictions over all matric potentials. Thus, soil characteristics Si and Cl were used together (SC) successively associated with one up to three of the following input data BD_{FC}, OC and θ_{FC}. Then, values of volumetric water content at water matric potentials of –1 (θ^p_1), –3.3 ($\theta^p_{3.3}$), –10 (θ^p_{10}), –33 (θ^p_{33}), –100 (θ^p_{100}), –330 (θ^p_{330}) and –1500 kPa (θ^p_{1500}) were predicted for the test dataset (Table 2).

2.2.3. Pedotransfer functions based on simple linear regression

Many studies have shown that the water content at particular values of water matric potential such as $\theta^m_{3.3}$ or θ^m_{1500} as input data increases the prediction performance of the water content at other values of matrix potential (e.g. Rawls et al., 1982; Schaap et al., 2001; Nemes et al., 2003; Twarakavi et al., 2009a, 2009b; Stumpp et al., 2009). However, $\theta^m_{3.3}$ and θ^m_{1500} are poorly available in numerous national soil databases (e.g. Johnston et al., 2003; Jolivet et al., 2006; Saby et al., 2014; Dobarco et al., 2019; Kristensen et al., 2019). Futhermore, Al Majou et al. (2008a) showed that the in situ volumetric water content at field capacity (θ_{FC}), which unfortunately is rarely available in soil databases, is a predictor leading to much better prediction of the water retention properties compared with the input data derived from the texture, organic carbon content and bulk density. As noted by Al Majou et al. (2008a), this was true regardless of the complexity of the PTFs developed.

On the basis of these results, we developed PTFs in the form of simple linear regression equations (SLR-PTFs) which predicted the volumetric water content at –1 ($\theta^p_{1.0}$), –3.3 ($\theta^p_{3.3}$), –10 (θ^p_{10}), –33 (θ^p_{33}), –100 (θ^p_{100}), –330 (θ^p_{330}) and –1500 kPa (θ^p_{1500}) matric potential using θ_{FC} as input data. These simple linear regression equations were developed and tested using the same training and test datasets used for the ANN-PTFs and SVM PTFs (Table 2). Since the bulk density at field capacity is not easily measurable, it was also predicted (BD^p_{FC}, g cm^{-3}) using the in situ gravimetric water content at field capacity (W^m_{FC}) measured for every horizon by establishing a regression equation as follows:

$$BD^p_{FC} = a + b(W_{FC}) \quad (1)$$

Then, BD^p_{FC} was used to compute a value of the in situ volumetric water content at field capacity (θ'_{FC}) for every horizon as follows:

$$\theta'_{FC} = W_{FC} \quad [a + b(W_{FC})] \quad (2)$$

This makes it possible to compare the performances of the PTFs when using θ_{FC} or θ'_{FC}. Finally, since the closeness of the relationships is potentially higher after texture stratification as shown by several earlier studies (Al Majou et al., 2007; Piedallu et al., 2011; Dobarco et al., 2019), we proceeded in the same way after stratification by texture according to the five texture classes of the soil map of the European Communities (Commission of the European Communities, 1985).

2.3. Criteria used to evaluate the performance of PTFs

The PTF performances for predicting soil water retention properties were compared using the root mean squared error (RMSE) and the coefficient of determination (R^2) which are commonly used in the literature (e.g. Pachepsky et al., 1996; Schaap and Leij, 1998; Wösten et al., 2001; D'Emilio et al., 2018; Singh et al., 2020; Kalumba et al., 2021) with:

$$RMSE = \left\{ \frac{1}{n \times l} \sum_{j=1}^{n} \sum_{i=1}^{l} \left(\theta_{i,j}^{p} - \theta_{i,j}^{m} \right)^2 \right\}^{1/2} \quad (3)$$

$$R^2 = 1 - \frac{\sum_{j=1}^{n} \sum_{i=1}^{l} \left(\theta_{i,j}^{p} - \theta_{i,j}^{m} \right)^2}{\sum_{j=1}^{n} \sum_{i=1}^{l} \left(\theta_{i,j}^{p} - \bar{\theta}_{i,j}^{m} \right)^2} \quad (4)$$

where $\theta_{i,j}^{p}$ ($cm^3\ cm^{-3}$) is the predicted water content at matric potential j for the horizon i, $\theta_{i,j}^{m}$ ($cm^3\ cm^{-3}$) is the measured water content at matric potential j for the horizon i, $\bar{\theta}_{j}^{m}$ ($cm^3\ cm^{-3}$) represents the average of the measured volumetric water content at the matric potential i, l is the number of matric potentials for each horizon (l = 7 in this study) and n is the number of horizons studied. The RMSE quantifies the root of the average bivariate variance between estimated and measured water content. It varies according to both the overall prediction bias and the overall prediction precision. The coefficient of determination (R^2) indicates the amount of variation in the data explained by the regression model, and it measures the strength of the linear relation between predicted and measured values.

3. Results and discussion

3.1. Characteristics of the soils studied

The mean basic properties of the horizons of the test dataset were close to those of the horizons used to develop the PTFs (Table 2). However, the horizons of the test dataset had a slightly smaller mean clay content (–1.4%), sand content (– 0.9%), organic carbon content (–0.7 g kg-1), mean CEC (–0.3 $cmol_+\ kg^{-1}$) and mean $CaCO_3$ content (21.5 g kg^{-1}) than in the training dataset (Table 2). Results also showed similar BD_{FC}^{m}, θ_{FC} and θ_{h}^{m} at the different matric potentials in the training and test datasets (Table 2).

The mean difference (MD) between θ_{FC} and successively $\theta_{3.3}$, θ_{10} and θ_{33} was computed as follows:

$$MD = \frac{1}{n} \sum_{i=1}^{n} \left(\theta_{FC,i} - \theta_{i,j}^{m} \right) \quad (5)$$

where $\theta_{FC,i}$ is the in situ volumetric water content at field capacity of the horizon i, $\theta_{i,j}^{m}$ is the measured water content at pressure head j for the horizon i, and n is the number of horizons (365 and 91 for the training and test dataset, respectively). The smallest absolute value of MD was recorded with θ_{10} for the whole training and test datasets with MD = 0.002 and –0.001 $cm^3\ cm^{-3}$, respectively (Fig. 1). The smallest absolute value MD was recorded also with θ_{10} whatever the texture (Table 3). The smallest and greatest absolute values of MD were recorded for the training dataset with θ_{10} for Fine texture (MD = –0.001 $cm^3\ cm^{-3}$) and Coarse texture (MD = 0.018 $cm^3\ cm^{-3}$), respectively (Table 3). For the test dataset, the smallest and greatest absolute values of MD were recorded with θ_{10} for Medium Fine and Very Fine textures (MD = 0.001 $cm^3\ cm^{-3}$) and Coarse texture (MD = 0.012 $cm^3\ cm^{-3}$), respectively (Table 3). These values of MD show that the closest water potential to that at field capacity was –10 kPa for the soils studied whatever their texture. They also show the lack of bias in terms of closeness of the field capacity between the training and test datasets when the soils were sampled.

3.2. Performance of the ANN-PTFs

When only one soil characteristic was used as input data, results showed that the smallest RMSE and highest R^2 were recorded with θ_{FC} (0.036 $cm^3\ cm^3$ and 0.85, respectively) (Table 4). Close RMSE and similar R^2 were recorded with SC as single imput data (0.037 $cm^3\ cm^3$ and 0.85, respectively). The best performance with two of the input data tested was recorded with SC and θ_{FC} (0.027 $cm^3\ cm^3$ and 0.92 for RMSE and R^2, respectively). With three or four of the input data tested, the performance did not increase (Table 4).

It was shown in the literature that the performance increased when points of the water retention curve were used among the set of input data, particularly when θ_{33}^{m} was used (Schaap et al., 1998; Schaap and Leij, 1998). For soils close to the soils studied, the performance of θ_{FC} was shown to be slightly greater than θ_{33}^{m} (Bruand et al., 1996) which is often associated with field capacity (Gaiser et al., 2000; Nemes et al., 2008; dos Santos et al., 2013; Ribeiro et al., 2018; Reichert et al., 2020). This is consistent with the increase in performance when θ_{FC} was used as input data even if it does not correspond to a volumetric water content at a well defined value of water potential (Table 4).

As recorded earlier, only a slight or no improvement in performance was observed when OC was included in the set of input data used (Nemes et al., 2003; Børgesen and Schaap, 2005; Haghverdi et al., 2012; D'Emilio et al., 2018). Results showed that there was no increase in the performance when OC was added to SC used as input data (0.037 $cm^3\ cm^{-3}$ and 0.84 for RMSE and R^2, respectively) (Table 4), On the other hand, they showed a slight increase in the performance when OC was added to SC and BD_{FC}^{m} used as input data (0.033 $cm^3\ cm^{-3}$ and 0.87 for RMSE and R^2, respectively) and to SC, BD_{FC}^{m} and θ_{FC} used as input data (0.027 $cm^3\ cm^{-3}$ and 0.92 for RMSE and R^2, respectively) (Table 4, Fig. 2). The slight or no contribution of OC as input data to improving the performance of the ANN-PTFs might explain why OC was not used as input data in PTFs based on ANNs when it is usually available in many soil databases (Schaap and Liej, 1998; Schaap et al., 1998; Rawls et al., 2003; Rawls et al., 2004; Stumpp et al., 2009; Vereecken et al., 2010; Batjes et al., 2020; Rudiyanto et al., 2021).

More generally, performances recorded with both the soils studied and ANN-PTFs were similar to or even higher than those discussed in the literature (Koekkoek and Bootlink, 1999; Merdun et al., 2006; D'Emilio et al., 2018; Singh et al., 2020; Kalumba et al., 2021) (Table 1).

3.3. Performance of the SVM-PTFs

Similar to what we found with the ANN-PTFs, those developed using SVM showed that when only one of the input data tested was used, the smallest RMSE and highest R^2 were recorded with θ_{FC} (0.026 $cm^3\ cm^{-3}$ and 0.74, respectively) (Table 5). Unlike what was found with the ANN-PTFs, the performance recorded with SC (0.038 $cm^3\ cm^{-3}$ and 0.67 for RMSE and R^2, respectively) was much smaller than with θ_{FC}. The best performance with two of the input data tested was recorded with SC and θ_{FC} but the value of RMSE was higher than when θ_{FC} was used as single input data (0.028 $cm^3\ cm^{-3}$ and 0.84 for RMSE and R^2, respectively) (Table 5). With three of the input data tested, the performances recorded were not increased with SC, BD_{FC}^{m} and OC and slightly increased with SC, BD_{FC}^{m} and θ_{FC} (0.027 $cm^3\ cm^{-3}$ and 0.84 for RMSE and R^2, respectively). There was no increase in the performances when the four input data SC, BD_{FC}^{m}, θ_{FC} and OC were used (0.027 $cm^3\ cm^{-3}$ and 0.84 for RMSE and R^2, respectively) (Table 5).

As shown with ANN-PTFs (Table 4), taking OC into account did not improve the performance whatever the number of input data tested (Table 4). As reported with ANN-PTFs (Table 4), a slight decrease in performance was even recorded when OC was added to SC and BD_{FC}^{m}or to SC, BD_{FC}^{m} and θ_{FC} when used as input data (Table 5, Fig. 2).

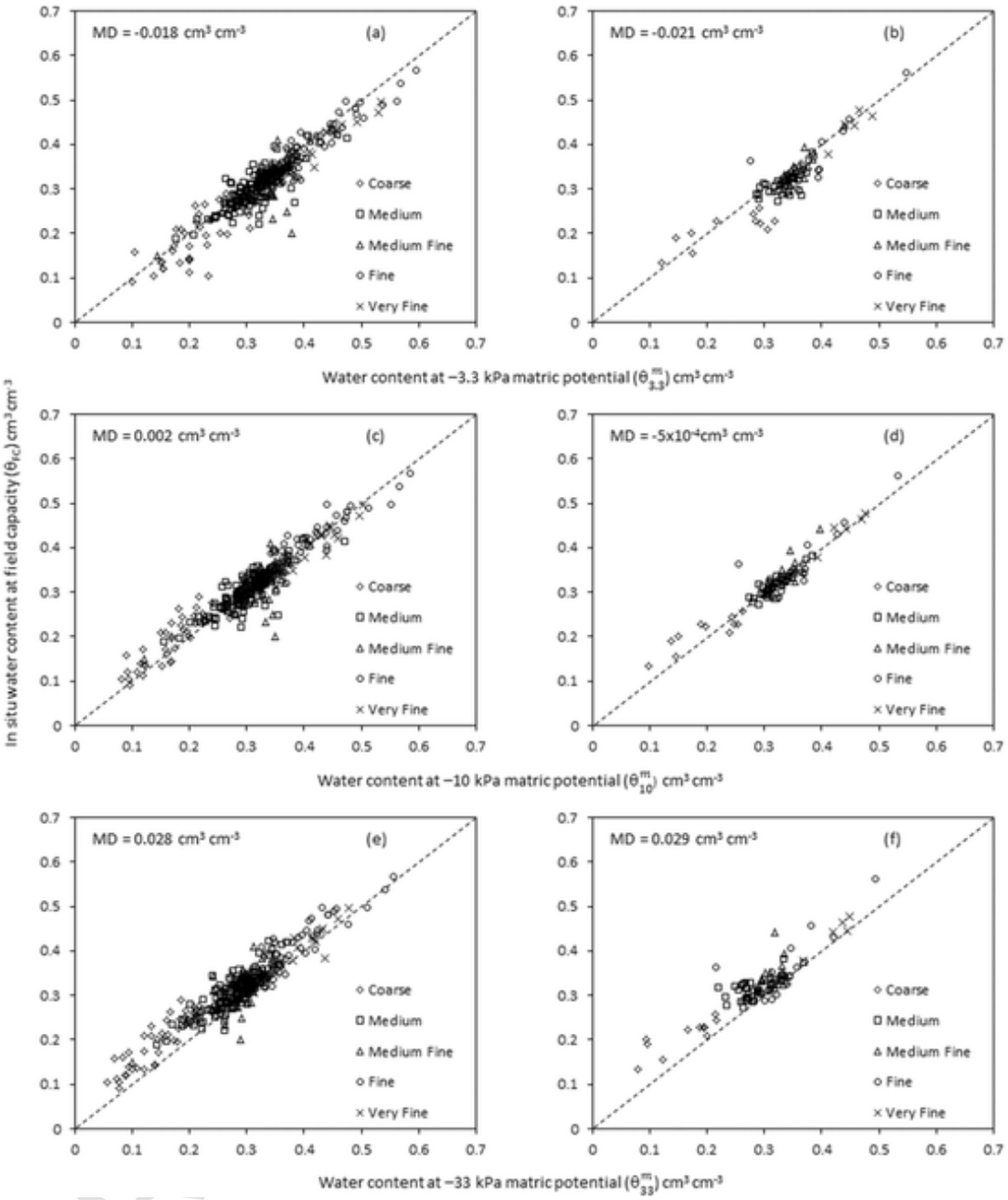

Fig. 1. Mean difference (MD) between the measured in situ volumetric water content at field capacity (θ_{FC}) and the measured volumetric water content at –3.3 kPa matric potential ($\theta^{m}_{3.3}$) for the training dataset (a) and test dataset (b), –10 kPa matric potential (θ^{m}_{10}) for the training dataset (c) and test dataset (d), and –33 kPa matric potential ($\theta^{m}_{3.3}$) for the training dataset (e) and test dataset (f) according to texture.

More generally, the comparison of the results recorded with the ANN-PTFs and SVM-PTFs showed no clear improvements in performance according to the type of PTF used (Tables 4 and 5), which is consistent with what Skalova et al. (2011) and Haghverdi et al. (2014) recorded. The results recorded with the ANN-PTFs and SVM-PTFs, however, clearly showed the relevance of θ_{FC} as input data to predict the water retention properties. As it is a point of the water retention curve, even if θ_{FC} does not correspond to a precise value of matric potential, its relevance as a predictor of other points of the water retention curve is consistent with results which showed the high relevance for such a prediction of θ^{m}_{33} and θ^{m}_{1500} (Schaap and Liej, 1998; Schaap et al., 2001; Nemes et al., 2003; Børgesen and Schaap, 2005; Stumpp et al., 2009; Twarakavi et al., 2009a, 2009b). However, θ_{FC} has rarely been used as input data whatever the type of PTF (Al Majou et al., 2008a) because it is seldom present in the databases, and is even absent in the WoSIS (Batjes et al., 2020).

3.4. Performance of SLR-PTFs

The coefficients a and b recorded for the regression equations between the volumetric water content at the different matric water potentials and θ_{FC} are given in Appendix A. The values of RMSE and R^2 recorded without any stratification were 0.035 $cm^3\ cm^{-3}$ and 0.85, respectively (Table 6). After stratification by texture, the latter being hand-feel determined (Thien, 1979; Ritchey et al., 2015) using the five texture classes of the soil map of the European Communities

Table 3
Mean difference (MD, $cm^3\ cm^{-3}$) between the volumetric water content at field capacity (θ^m_{FC}) and successively $\theta_{3.3}$ ($MD_{\theta 3.3}$), θ_{10} ($MD_{\theta 10}$) and θ_{33} ($MD_{\theta 33}$) according to the texture class for the training and test datasets.

	Mean Difference (MD $cm^3\ cm^{-3}$)		
	$MD_{\theta 3.3}$	$MD_{\theta 10}$	$MD_{\theta 33}$
	Training dataset (n = 365)		
Coarse (n = 45)	– 0.019	0.018	0.048
Medium (n = 121)	– 0.016	0.002	0.027
Medium Fine (n = 102)	– 0.019	– 0.002	0.027
Fine (n = 82)	– 0.018	– 0.001	0.021
Very Fine (n = 15)	– 0.029	– 0.015	0.007
	Test dataset (n = 91)		
Coarse (n = 45)	– 0.028	0.012	0.049
Medium (n = 121)	– 0.025	– 0.003	0.032
Medium Fine (n = 102)	– 0.018	0.001	0.025
Fine (n = 82)	– 0.020	– 0.006	0.020
Very Fine (n = 15)	– 0.011	0.001	0.018

Table 4
Root mean squared error (RMSE) and coefficient of determination (R^2) recorded with the PTFs based on ANN according to the type and number of input data.

Input data	Descriptive statistics of the relationship between measured and predicted water content	
	RMSE $cm^3\ cm^{-3}$	R^2
	Training dataset (n = 365)	
SC	0.030	0.88
BD^m_{FC}	0.059	0.55
OC	0.063	0.49
θ_{FC}	0.035	0.87
SC, BD^m_{FC}	0.028	0.90
SC, OC	0.030	0.90
SC, θ_{FC}	0.022	0.94
SC, BD^m_{FC}, OC	0.028	0.90
SC, BD^m_{FC}, θ_{FC}	0.022	0.95
SC, BD^m_{FC}, θ_{FC}, OC	0.020	0.95
	Test dataset (n = 91)	
SC	0.037	0.85
BD^m_{FC}	0.065	0.52
OC	0.066	0.49
θ_{FC}	0.036	0.85
SC, BD^m_{FC}	0.035	0.86
SC, OC	0.037	0.84
SC, θ_{FC}	0.027	0.92
SC, BD^m_{FC}, OC	0.033	0.87
SC, BD^m_{FC}, θ_{FC}	0.027	0.91
SC, BD^m_{FC}, θ_{FC}, OC	0.027	0.91

SC: silt (0.02 – 0.050 mm) and clay (< 2 μm) content; BD^m_{FC}: bulk density measured at field capacity; OC: organic carbon content; θ_{FC}: in situ volumetric water content measured at field capacity.

(Commission of the European Communities, 1985), the performances of the SLR-PTFs using θ_{FC} as input data were better than with those established without stratification by texture (0.031 $cm^3\ cm^{-3}$ and 0.88 for RMSE and R^2, respectively) (Table 6). We note also that the performances of the SLR-PTFs using θ_{FC} as single input data after stratification by texture were better than those recorded with the ANN-PTFs and θ_{FC} as single input data (Tables 4 and 6). When θ_{FC} was used as single input data, the comparison of the SVM-PTFs with SLR-PTFs showed that the RMSE and R^2 were higher for the latter (RMSE = 0.031 $cm^3\ cm^{-3}$ and R^2 = 0.88) (Tables 5 and 6).

Our objective being to predict the water retention properties using a soil characteristic that was easy to measure and that enabled easy measurement of performances, we established regression equations between BD^m_{FC} and W^m_{FC} to avoid the measurement of the bulk density (Table 7). Then, coefficients a and b of the regression equations between the volumetric water content at the different matric water potentials (θ^m_h) and the in situ volumetric water content at field capacity (θ'_{FC}) which used BD^p_{FC} according to Eq. (1) were calculated (Appendix B). Results showed that the RMSE and R^2 values recorded without any stratification were 0.041 $cm^3\ cm^{-3}$ and 0.80, respectively (Table 6). As expected, the performances were smaller with θ'_{FC}than with θ_{FC} without any stratification (RMSE = 0.041 $cm^3\ cm^{-3}$ and R^2 = 0.80) and after stratification by texture (RMSE = 0.035 $cm^3\ cm^{-3}$ and R^2 = 0.86) (Table 6). After stratification by texture, the performances were less than those recorded with the ANN-PTFs and SVM-PTFs studied but still close (Tables 4, 5 and 6, Fig. 2).

3.5. Implications for end-users of water retention properties of soils

Our results show that not only the use of the in situ volumetric water content at field capacity is a relevant soil characteristic when combined with other soil characteristics (Tables 3 and 4) but also that it can be used as single predictor of the water retention properties of soils (Table 6). While the gravimetric or volumetric water content at field capacity is most of the time absent from the soil databases (Batjes et al., 2020), which limits the use of PTFs having the form of simple linear regressions as developed in this study (Appendix A and B), it can be easily determined without using laboratory equipment. The bulk density and in situ gravimetric water content at field capacity can be easily determined together using a soil core sampler in the field and then by oven-drying at 105 °C the soil samples collected when the soil was close to field capacity (Reeve et al., 1977; Twarakavi et al., 2009a, 2009b). As the most accurate predictions were recorded after stratification by texture using the five textures of the European Communities (Commission of the European Communities, 1985) (Table 5), the latter can be easily determined by hand-feel while collecting the soil samples to determine the gravimetric water content (Food and Agriculture Organisation, 1990; Richer-de-Forges et al., 2022). Thus, knowing W^m_{FC} and BD^m_{FC}, depending on whether the texture is known or not, the volumetric water contents $\theta^p_{1.0}$, $\theta^p_{3.3}$, θ^p_{10}, θ^p_{33}, θ^p_{100}, θ^p_{330} and θ^p_{1500} can be predicted using θ_{FC} as indicated in Table 6 and the parameters of the SLR-PTFs given in Appendix A (Fig. 3). If W^m_{FC} is known but not BD^m_{FC}, depending on whether the texture is known or not, the volumetric water contents $\theta^p_{1.0}$, $\theta^p_{3.3}$, θ^p_{10}, θ^p_{33}, θ^p_{100}, θ^p_{330} and θ^p_{1500} can be predicted using θ'_{FC} computed as indicated in Table 6 and the parameters of the SLR-PTFs given in Appendix B (Fig. 3).

As the water content at field capacity isclose to the water content at a matric potential of –10 kPa as discussed above, it can be considered as a point of the water retention curve, thus explaining the performance of the SLR-PTFs when it is used as single predictor of the water content for other points of the water retention curve. Rawls et al. (1982) and Paydar and Cresswell (1996) showed indeed that using one or more measured points of the water retention curve improved the prediction of the whole curve when compared to its prediction with particle size distribution, bulk density and organic carbon content.

If the ability of W^m_{FC} to predict the entire water retention curve has been shown for a wide range of French soils, one can wonder whether the SLR PTFs that have been developed and that appeared to be regionally relevant are also relevant on a larger scale. Regarding this point, Al Majou et al. (2021) showed for Syrian clayey soils the relevance of W^m_{FC} to predict their water retention properties. Moreover, D'Angelo et al. (2014) showed the relevance of W^m_{FC} to discuss the water retention properties of Chinese red clay soils which were recognaized as being

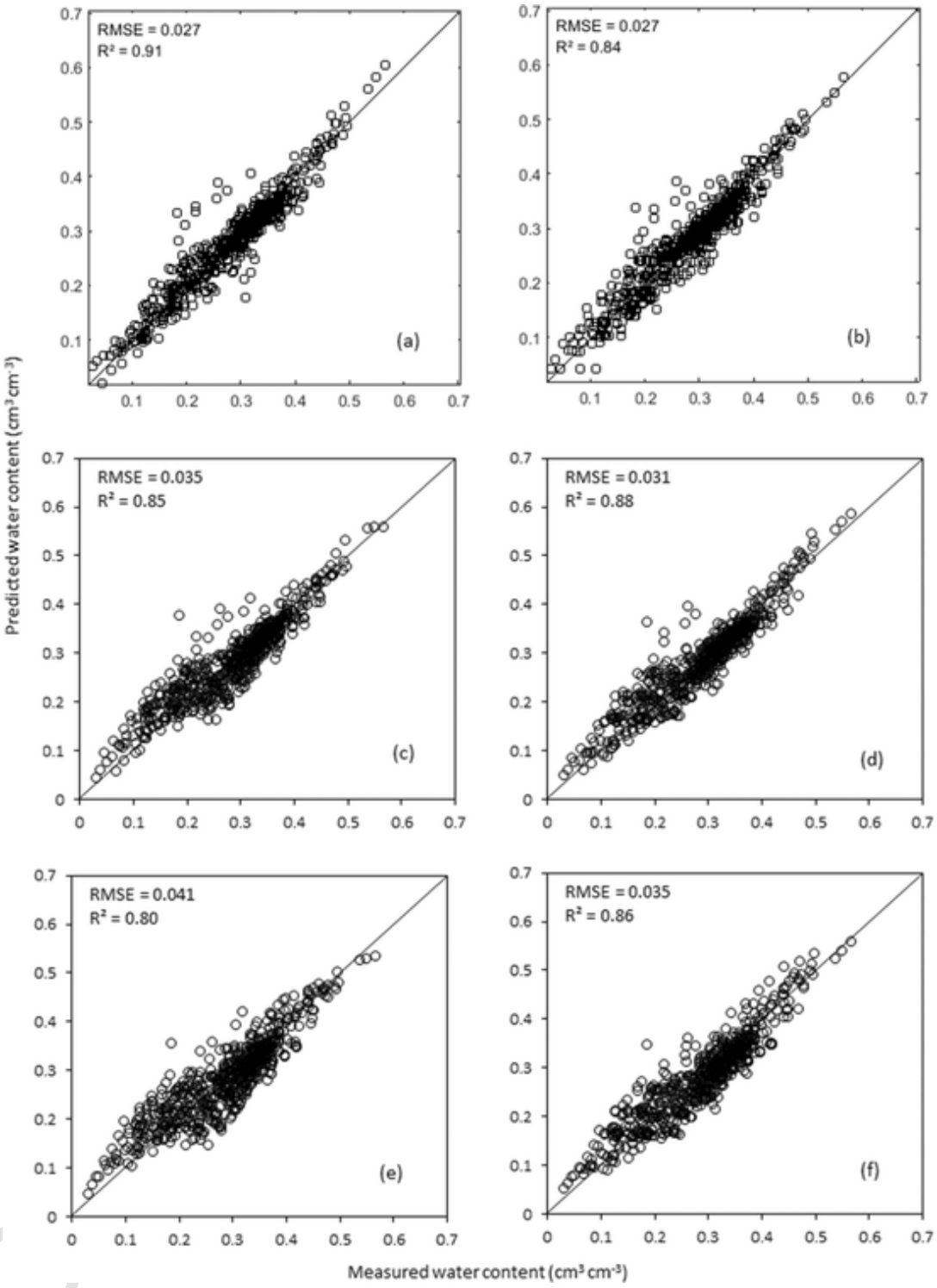

Fig. 2. Comparison of measured and predicted volumetric water content on the test dataset using ANN-PTFs with SC, $BD^{p}_{FC}$and θ_{FC} as predictors (a), SVM-PTFs with SC, $BD^{p}_{FC}$and θ_{FC} as predictors (b), SLR-PTFs with θ_{FC} as predictor without any stratification (c), SLR-PTFs with θ_{FC} as predictor after stratification by texture (d), SLR-PTFs with θ'_{FC} as predictor without any stratification (e), SLR-PTFs with θ_{FC} as predictor after stratification by texture (f).

highly sensitive to drought. We can then infer from our results the interest of using W^{m}_{FC} as single predictor of the water retention properties of soils on a much broader scale than for the territory from which the soils studied come.

4. Conclusion

For the soils studied, our results showed the relevance of using the in situ gravimetric water content at field capacity to calculate the volumetric water content at field capacity, whether the bulk density was

Table 5
Root mean squared error (RMSE) and coefficient of determination (R^2) recorded with the PTFs based on SVM according to the type and number of input data.

Input data	Descriptive statistics of the relationship between measured and predicted water content	
	RMSE $cm^3\ cm^{-3}$	R^2
	Training dataset (n = 365)	
SC	0.040	0.71
BD_{FC}	0.069	0.16
OC	0.075	0.02
θ_{FC}	0.026	0.75
SC, BD^m_{FC}	0.039	0.76
SC, OC	0.039	0.72
SC, θ_{FC}	0.028	0.85
SC, BD^m_{FC}, OC	0.039	0.73
SC, BD^m_{FC}, θ_{FC}	0.028	0.86
SC, BD^m_{FC}, θ_{FC}, OC	0.028	0.86
	Test dataset (n = 91)	
SC	0.038	0.67
BD^m_{FC}	0.065	0.14
OC	0.070	0.02
θ_{FC}	0.026	0.74
SC, BD^m_{FC}	0.037	0.73
SC, OC	0.039	0.66
SC, θ_{FC}	0.028	0.84
SC, BD^m_{FC}, OC	0.039	0.67
SC, BD^m_{FC}, θ_{FC}	0.027	0.84
SC, BD^m_{FC}, θ_{FC}, OC	0.027	0.84

SC: silt (0.02 – 0.050 mm) and clay (< 2 μm) content; BD^m_{FC}: bulk density measured at field capacity; OC: organic carbon content; θ_{FC}: volumetric water content measured at field capacity·

Table 6
Root mean squared error (RMSE) and coefficient of determination (R^2) recorded with the PTFs using the in situ volumetric water content at field capacity.

Input data	Descriptive statistics of the relationship between measured and predicted bulk density	
	RMSE $cm^3\ cm^{-3}$	R^2
	Without any stratification	
θ_{FC} with $\theta_{FC} = W^m_{FC} \times BD^m_{FC}$	0.035	0.85
$\theta'_{FC}$with $\theta'_{FC} = W^m_{FC}\left[a + b(W^m_{FC})\right]$	0.041	0.80
	After stratification by texture	
θ_{FC} with $\theta_{FC} = W^m_{FC} \times BD^m_{FC}$	0.031	0.88
θ'_{FC} with $\theta'_{FC} = W^m_{FC}\left[a + b(W^m_{FC})\right]$	0.035	0.86

θ_{FC}, the in situ volumetric water content at field capacity based on the measured in situ gravimetric water content at field capacity (W_{FC}) and the measured bulk density at field capacity (BD^m_{FC}); θ'_{FC}, the in situ volumetric water content at field capacity obtained by using the measured in situ gravimetric water content at field capacity (W^m_{FC}) and the predicted bulk density at field capacity (BD^p_{FC}) with $BD^p_{FC} = a + b(W^m_{FC})$.

measured or not, using simple regression equations. They showed also that the in situ volumetric water content at field capacity was close to that measured in the laboratory at –10 kPa matric potential which can then be considered as a point of the water retention curve, thus explaining its high capacity to predict the water retention properties.

Table 7
Regression coefficients and coefficient of determination R^2 recorded for the regression equations relating BD^m_{FC} and W^m_{FC}.

		Regression coefficients and coefficient of determination
		Without any stratification
All textures together (n = 365)	A	1.862 ***
	B	-1.627 ***
	R^2	0.52
		After stratification by texture
Very Fine (n = 15)	A	2.176 ***
	B	-2.613 ***
	R^2	0.87
Fine (n = 82)	A	1.870 ***
	B	-1.597 ***
	R^2	0.75
Medium Fine (n = 102)	A	1.971 ***
	B	-2.223 ***
	R^2	0.36
Medium (n = 121)	A	2.094 ***
	B	-2.671 ***
	R^2	0.57
Coarse (n = 45)	A	1.786 ***
	B	-1.337
	R^2	0.20

$BD_{FC} = a + b\ (W_{FC})$ with BD_{FC}, the bulk density measured at field capacity, W_{FC}, the gravimetric water content measured at field capacity, and a and b, the regression coefficients. *** P = 0.001, ** P = 0.01, * P = 0.05.

With PTFs using ANN, the best performances were recorded when the in situ volumetric water content at field capacity was used as input data combined with both the silt and the clay content. With PTFs using SVM, the smallest root mean squared error was recorded when the in situ volumetric water content at field capacity was used as single input data. As for the coefficient of determination, it increased with the number of soil characteristics associated with the in situ volumetric water content at field capacity. Our results also showed that the PTFs having the form of simple linear regression equations and using the in situ volumetric water content at field capacity as single predictor after stratification by texture performed better than the PTFs using ANNs that we established with a single soil characteristic as input data. Better performances were recorded with PTFs based on ANN when several soil characteristics were associated, the best perfomances being recorded when the in situ volumetric water content at field capacity was used associated with both silt and clay content and bulk density at field capacity as input data.

Comparison of PTFs having the form of simple linear regression equations with PTFs based on SVM showed that the latter performed slightly better than PTFs having the form of simple linear regressions after stratification by texture but that the coefficient of determination was smaller when the in situ volumetric water content at field capacity was used as single predictor. Use of a predicted value of the bulk density at field capacity to obtain a value of in situ volumetric water content at field capacity led to poorer performances of the PTFs having the form of simple regression equations but after stratification by texture they remained close to those recorded with PTFs based on ANN or SVM. Finally, our results showed that associating the carbon organic carbon content to the input data did not increase the perfomances of the PTFs based on ANN or SVM.

Declaration of Competing Interest

The authors declare that they have no known competing financial interests or personal relationships that could have appeared to influence the work reported in this paper.

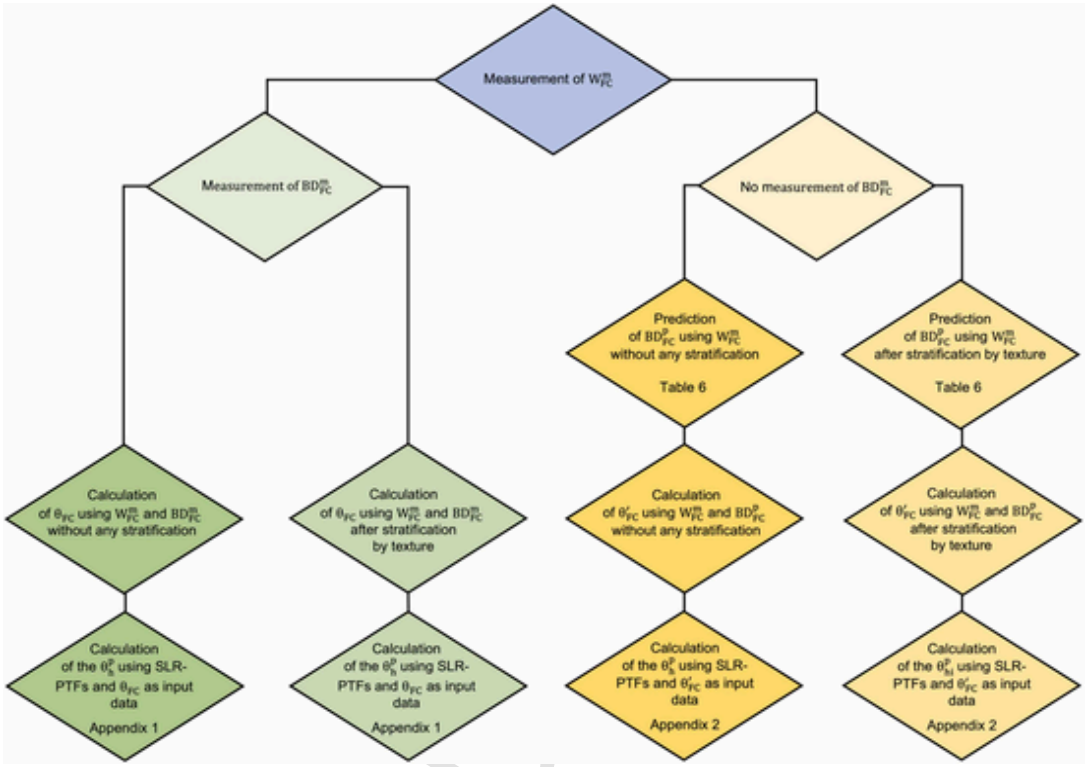

Fig. 3. Flowchart illustrating the prediction of the water retention properties of a horizon using the measured in situ water content at field capacity (W^m_{FC}).

Data Availability

Data will be made available on request.

Acknowledgments

The authors would like to thank the LabEx VOLTAIRE (LABX-100–01) project for its support.

Appendix A

See Table A1.

APPENDIX B.

See Table B1.

Table A1
Regression coefficients a and b, and coefficient of determination R^2 recorded for the PTFs established by simple regression by using the in situ volumetric water content measured at field capacity (θ_{FC}) without any stratification by texture and after stratification by texture.

		Matric potential (kPa)						
		-1	-3.3	-10	-33	-100	-330	-1500
		Without any stratification						
All textures together	a	0.0845***	0.0425***	-0.0015	-0.0275***	-0.0566***	-0.0550***	-0.0606***
(n = 365)	b	0.8495***	0.9222***	0.9998***	0.9997***	1.0036***	0.8778***	0.7854***
	R^2	0.79	0.86	0.89	0.88	0.83	0.70	0.58
		After stratification by texture						
Very Fine	a	-0.0871	0.0093	0.0397	0.0579	0.0867*	0.2220***	0.1199*
(n = 15)	b	1.3300***	1.0489***	0.9403***	0.8393***	0.7325***	0.3234*	0.5081***
	R^2	0.92	0.91	0.90	0.85	0.83	0.37	0.61
Fine	a	0.0491**	0.0326*	0.0125	0.0174	0.0041	0.0385*	0.0635**
(n = 82)	b	0.9614***	0.9604***	0.9682***	0.8973***	0.8819***	0.6942***	0.5384***
	R^2	0.86	0.90	0.89	0.86	0.86	0.72	0.48
Medium Fine	a	0.1844***	0.1766***	0.1645***	0.1180***	0.0634	0.0684	0.0625
(n = 102)	b	0.5301***	0.5106***	0.4978***	0.5511***	0.5900***	0.4376***	0.3451**
	R^2	0.31	0.38	0.38	0.43	0.26	0.12	0.07
Medium	a	0.1170***	0.0773***	0.0510***	0.0370**	0.0234	0.0686**	0.0923***
(n = 121)	b	0.7184***	0.7935***	0.8226***	0.7842***	0.7488***	0.4602***	0.2417**
	R^2	0.52	0.64	0.70	0.71	0.61	0.27	0.06
Coarse	a	0.1425***	0.0793***	0.0006	-0.0164	-0.0232	-0.0242	-0.0143
(n = 45)	b	0.5845***	0.7031***	0.9041***	0.8436***	0.7465***	0.6425***	0.4990***
	R^2	0.40	0.59	0.78	0.79	0.75	0.69	0.61

$\theta_h^p = a + b\,(\theta_{FC})$ with θ_h^p, the volumetric water content predicted at matric potential -h, θ_{FC}, the in situ volumetric water content measured at field capacity and corresponding to $\theta_{FC} = W_{FC} \times BD_{FC}$. *** P = 0.001, ** P = 0.01, * P = 0.05.

Table B1
Regression coefficients a and b, and coefficient of determination R^2 recorded for the PTFs established by simple regression by using the volumetric water content predicted at field capacity (θ'_{FC}) without any stratification and after stratification by texture.

		Matric potential (kPa)						
		-1	-3.3	-10	-33	-100	-330	-1500
		Without any stratification						
All textures together	a	0.0823***	0.0433***	0.0019	− 0.0196*	− 0.0426***	− 0.0393***	− 0.0465***
(n = 365)	b	0.8565***	0.920***	0.9895***	0.9749***	0.9594***	0.8285***	0.7409***
	R^2	0.76	0.82	0.83	0.80	0.72	0.60	0.50
		After stratification by texture						
Very Fine (n = 15)	a	− 0.0684	0.0101	0.0502	0.0785	0.1109	0.2297**	0.1367*
	b	1.2836***	1.0469***	0.9142***	0.7881***	0.6729***	0.3046*	0.4664**
	R^2	0.72	0.76	0.71	0.63	0.59	0.28	0.44
Fine (n = 82)	a	0.0478*	0.0298	0.0118	0.0197	0.0077	0.0478*	0.0807**
	b	0.9655***	0.9681***	0.9705***	0.8915***	0.8727***	0.6696***	0.4931***
	R^2	0.81	0.84	0.83	0.79	0.78	0.62	0.37
Medium Fine (n = 102)	a	0.1887***	0.1874***	0.1746***	0.1404***	0.1189**	0.1396**	0.1151*
	b	0.5168***	0.4770***	0.4664***	0.4816***	0.4179**	0.2168	0.1822
	R^2	0.23	0.25	0.26	0.26	0.10	0.02	0.02
Medium (n = 121)	a	0.0853***	0.0587**	0.0398*	0.0423*	0.0457*	0.0933***	0.1179***
	b	0.8244***	0.8556***	0.8599***	0.7664***	0.6739***	0.3774***	0.1557
	R^2	0.56	0.61	0.63	0.56	0.40	0.15	0.02
Coarse (n = 45)	a	0.1420***	0.0848***	0.0080	− 0.0066	− 0.0121	− 0.0137	− 0.0051
	b	0.5866***	0.6760***	0.8677***	0.7948***	0.6915***	0.5911***	0.4534***
	R^2	0.37	0.50	0.66	0.65	0.59	0.54	0.46

$\theta^p_h = a + b\,(\theta'_{FC})$ with θ^p_h, the volumetric water content predicted at matric potential -h, θ'_{FC}, the in situ volumetric water content at field capacity corresponding to $\theta'_{FC} = W_{FC} \times BD^p_{FC}$ with $BD^p_{FC} = a + b\,(W_{FC})$ (see Table 6). *** P = 0.001, ** P = 0.01, * P = 0.05.

References

Al Majou, H., Bruand, A., Duval, O., Cousin, I., 2007. Variation of the water retention properties of soils: validity of class-pedotransfer functions. Comptes Rendus Geosci. 339, 632–639.

Al Majou, H., Bruand, A., Duval, O., 2008a. Use of in situ volumetric water content at field capacity to improve prediction of soil water retention properties. Can. J. Soil Sci. 88, 533–541.

Al Majou, H., Bruand, A., Duval, O., Le Bas, C., Vautier, A., 2008b. Prediction of soil water retention properties after stratification by combining texture, bulk density and the type of horizon. Soil Use Manag. 24, 383–391.

Al Majou, H., Hassani, B., Bruand, A., 2018. Transferability of continuous- and class-pedotransfer functions to predict water retention properties of semiarid Syrian soils. Soil Use Manag 34, 354–369.

Al Majou, H., Muller, F., Penhoud, P., Bruand, A., 2021. Prediction of water retention properties of Syrian clayey soils. Arid Land Res. Manag. 36, 125–144.

Amorim, R.S.S., Albuquerque, J.A., Couto, E.G., Kunz, M., Rodrigues, M.F., da Silva, L.D.M., Reichert, J.M., 2022. Water retention and availability in Brazilian Cerrado (neotropical savanna) soils under agricultural use: Pedotransfer functions and decision tree. Soil Till. Res. 224, 105485.

Babaeian, E., Homaee, M., Vereecken, H., Montzka, C., Norouzi, A.A., van Genuchten, M.T., 2015. A comparative study of multiple approaches for predicting the soil-water retention curve: hyperspectral information vs. basic soil properties. Soil Sci. Soc. Am. J. 79, 1043–1058.

Bagnall, D.K., Morgan, C.L.S., Cope, M., Bean, G.M., Cappellazzi, S., Greub, K., Liptzin, D., Norris, C.L., Rieke, E., Tracy, P., Aberle, E., Ashworth, A., Bañuelos Tavarez, O., Bary, A., Baumhardt, R.L., Borbón Gracia, A., Brainard, D., Brennan, J., Briones Reyes, D., Bruhjell, D., Carlyle, C., Crawford, J., Creech, C., Culman, S., Deen, W., Dell, C., Derner, J., Ducey, T., Duiker, S.W., Dyck, M., Ellert, B., Entz, M., Espinosa Solorio, A., Fonte, S.J., Fonteyne, S., Fortuna, A.M., Foster, J., Fultz, L., Gamble, A.V., Geddes, C., Griffin-LaHue, D., Grove, J., Hamilton, S.K., Hao, X., Hayden, Z.D., Howe, J., Ippolito, J., Johnson, G., Kautz, M., Kitchen, N., Kumar, S., Kurtz, K., Larney, F., Lewis, K., Liebman, M., Lopez, Ramirez, A., Machado, S., Maharjan, B., Martinez, Gamiño, M.A., May, W., McClaran, M., McDaniel, M., Millar, N., Mitchell, J.P., Moore, P.A., Moore, A., Mora, Gutiérrez, M., Nelson, K.A., Omondi, E., Osborne, S., Osorio Alcalá, L., Owens, P., Pena-Yewtukhiw, E.M., Poffenbarger, H., Ponce Lira, B., Reeve, J., Reinbott, T., Reiter, M., Ritchey, E., Roozeboom, K.L., Rui, I., Sadeghpour, A., Sainju, U.M., Sanford, G., Schillinger, W., Schindelbeck, R.R., Schipanski, M., Schlegel, A., Scow, K., Sherrod, L., Sidhu, S., Solís Moya, E., Luce, M.St, Strock, J., Suyker, A., Sykes, V., Tao, H., Trujillo Campos, A., Van Eerd, L.L., Verhulst, N., Vyn, T.J., Wang, Y., Watts, D., Wright, D., Zhang, T., Honeycutt, C.W., 2022. Carbon-sensitive pedotransfer functions for plant available water. In: Soil Sci. Soc. Am. J, 86. pp. 612–629.

Baize, D., 2000. Guide des analyses en pédologie. INRA Paris.

Baker, L., 2008. Development of class pedotransfer functions of soil water retention: a refinement. Geoderma 144, 225–230.

Batjes, N.H., Ribeiro, E., van Oostrum, A., 2020. Standardised soil profile data to support global mapping and modelling (WoSIS snapshot 2019). Earth Syst. Sci. Data 12, 299–320.

Børgesen, C.D., Schaap, M.G., 2005. Point and parameter pedotransfer functions for water retention prediction for Danish soils. Geoderma 127, 154–167.

Botula, Y.D., Van Ranst, E., Cornelis, W.M., 2014. Pedotransfer functions to predict water retention for soils of the humid tropics: a review. Rev. Bras. Ciênc. Solo 38, 679–698.

Bouma, J., 1989. Land qualities in space and time. p 3–13. In J. Bouma and A.K. Bregt (ed.) Proc. ISSS Symp. On land qualities in space and time, Wageningen, the Netherlands. 22–26 Aug. 1988. Pudoc. Wageningen.

Bouma, J., van Lanen, H.A.J., 1987. Transfer functions and threshold values: from soil characteristics to land qualities. p 106–111. In: Beek K.J., P.A. Burrough and D.E. McCormack (eds.), Proc. ISSS/SSSA Workshop on Quantified Land Evaluation Procedures. Int. Inst. for Aerospace Surv. and Earth Sci., Publ. No 6, Enschede, The Netherlands.

Briggs, L.J., Lane, J.W.M., 1907. The Moisture Equivalents of Soils. (U.S. Department of Agriculture Bureau of Soils. Bulletin). U.S. Government Printing Office, p. 23.

Bruand, A., Tessier, D., 2000. Water retention properties of the clay in soils developed on clayey sediments: significance of parent material and soil history. Eur. J. Soil Sci. 51, 679–688.

Bruand, A., Baize, D., Hardy, M., 1994. Prediction of water retention properties of clayey soils: validity of relationships using a single soil characteristic. Soil Use Manag. 10, 99–103.

Bruand, A., Duval, O., Gaillard, H., Darthout, R., Jamagne, M., 1996. Variabilité des propriétés de rétention en eau des sols: importance de la densité apparente. Etude Et. Gest. Des. Sols 3, 27–40.

Bruand, A., Pérez Fernandez, P., Duval, O., 2003. Use of class pedotransfer functions based on texture and bulk density of clods to generate water retention curves. Soil Use Manag. 19, 232–242.

Bruand, A., Duval, O., Cousin, I., 2004. Estimation des propriétés de rétention en eau des sols à partir de la base de données SOLHYDRO: Une première proposition combinant le type d'horizon, sa texture et sa densité apparente. Etude Et. Gest. Des. Sols 11, 323–332.

Ciesielski, H., Sterckeman, T., 1997. Determination of cation exchange capacity and exchangeable cations in soils by means of cobalt hexamine trichloride. Eff. Exp. Cond. Agron. 17, 1–7.

Commission of the European Communities, 1985. Soil map of the European Communities. Scale 1:1 000 000, CEC-DGVI, Luxembourg.

Cornelis, M., Ronsyn, J., Van Meirvenne, M., Hartmann, R., 2001. Evaluation of pedotransfer functions for predicting the soil moisture retention curve. Soil Sci. Soc. Am. J. 65, 638–648.

Cueff, S., Coquet, Y., Aubertot, J.N., Bel, L., Pot, V., Allettuo, L., 2021. Estimation of soil water retention in conservation agriculture using published and new pedotransfer functions. Soil Till. Res. 209, 104967.

D'Emilio, A., Aiello, R., Consoli, S., Vanella, D., Iovino, M., 2018. Artificial neural networks for predicting the water retention curve of Sicilian agricultural soils. Water 10, 1431.

D'Angelo, B., Bruand, A., Qin, J.T., Peng, X.H., Hartmann, C., Sun, B., Hao, H.T., Rozenbaum, O., Muller, F., 2014. Origin of the high sensitivity of Chinese red clay soils to drought: Significance of the clay characteristics. Geoderma 223, 46–53.

De Jong, R., Loebel, K., 1982. Empirical relations between soil components and water

retention at 1/3 and 15 atmospheres. Can. J. Soil Sci. 62, 343–350.
Demuth, H., Beale, M. 2000. Neural network toolbox for use with MATLAB. User guide. The MathWorks, Inc., Natick, MA.
Dobarco, M.R., Cousin, I., Le Bas, C., Martin, M.P., 2019. Pedostransfer functions for predicting available water capacity in French soils, their applicability domain and associated uncertainty. Geoderma 336, 81–95.
Food and Agriculture Organisation, 1990. Guidelines for Soil Description, third ed. FAO/ISRIC, Rome.
Gaiser, J., Graef, F., Cordiero, J.C., 2000. Water retention of soils with contrasting clay mineral composition in semi-arid tropical regions. Austral J. Soil Sci. 38 (3), 523–536.
Gupta, S.C., Larson, W.E., 1979. Estimating soil water retention characteristics from particle size distribution, organic matter percent and bulk density. Water Resour. Res. 15, 1633–1635.
Haghverdi, A., Cornelis, W.M., Ghahraman, B., 2012. A pseudo-continuous neural approach for developing water retention pedotransfer functions with limited data. J. Hydrol. 442, 46–54.
Haghverdi, A., Ozturk, H.S., Cornelis, W.M., 2014. Revisiting the pseudo continuous pedotransfer function concept: impact of data quality and data mining method. Geoderma 226, 31–38.
IUSS Working Group WRB, 2015. World Reference Base for Soil Resources 2014, update 2015. International soil classification system for naming soils and creating legends for soil maps. World Soil Resources Reports No 106. Rome, Italy: Food and Agricultural Organization.
Jana, R.B., Mokanty, B.P., Springer, E.P., 2007. Multiscale pedotransfer functions for soil water retention. Vadose Zone J. 6, 868–878.
Johnston, R.M., Barry, S.J., Bleys, E., Bui, E.N., Moran, C.J., Simon, D.A.P., Carlile, P., McKenzie, N.J., Henderson, B.L., Chapman, G., Imhoff, M., Maschmedt, D., Howe, D., Grose, C., Schoknecht, N., Powell, B., Grundyj, M., 2003. ASRIS: the database. Aust. J. Soil Res. 41, 1021–1036.
Jolivet, C., Arrouays, D., Boulonne, L., Ratié, C., Saby, N., 2006. Le réseau de mesure de la qualité des sols. Etude Et. Gest. Des. Sols 13, 149–164.
Kalumba, M., Bamps, B., Nyambe, I., Dondeyne, S., Van Orshoven, J., 2021. Development and functional evaluation of pedotransfer function for soil hydraulic properties for the Zambezi River Basin. Eur. J. Soil Sci. 72, 1559–1574.
Khlosi, M., Alhamdoosh, M., Douaik, A., Gabiels, D., Cornelis, W.M., 2016. Enhanced pedotransfer functions with support vector machines to predict water retention of calcareous soils. Eur. J. Soil Sci. 67, 276–284.
Koekkoek, E.J.W., Bootlink, H., 1999. Neural network models to predict soil water retention. Eur. J. Soil Sci. 50, 489–495.
Kristensen, J.A., Balstrøm, T., Jones, R.J.A., Jones, A., Montanarella, L., Panagos, P., Breuning-Madsen, H., 2019. Development of a harmonised soil profile analytical database for Europe: a resource for supporting regional soil management. Soil 5, 289–301.
Kværnø, S.H., Haugen, L.E., 2011. Performance of pedotransfer functions predicting soil water characteristics of soils in Norway. Agric. Scand. Sect. B Soil Plant Sci. 61, 264–280.
Lamorski, K., Pachepsky, Y., Slawihski, C., Walezak, R.T., 2008. Using support vector machines to develop pedotransfer functions for water retention of soils in Poland. Soil Sci. Soc. Am. J. 72, 1243–1247.
van Looy, K., Bouma, J., Herbst, M., Koestel, J., Minasny, B., Mishra, U., Montzka, C., Nemes, A., Pachepsky, Y.A., Padarian, J., Schaap, M.G., Toth, B., Verhoef, A., Vanderborght, J., van der Ploeg, M.J., Weihermuller, L., Zacharias, S., Zhang, Y.G., Vereecken, H., 2017. Pedotransfer functions in earth system science: challenges and perspectives. Rev. Geophys. 55, 1199–1256.
Merdun, H., Çinar, Ö., Meral, R., Apan, M., 2006. Comparison of artificial neural network and regression pedotransfer functions for prediction of soil water retention and saturated hydraulic conductivity. Soil Till. Res. 90, 108–116.
Minasny, B., Hartemink, A.F., 2011. Predicting soil properties in the tropics. Earth Sci. Rev. 106, 52–62.
Minasny, B., McBratney, A.B., Bristow, K.L., 1999. Comparison of different approaches to the development of pedotransfer functions for water-retention curves. Geoderma 93, 225–253.
Nemes, A., Schaap, M.G., Wösten, J.H.M., 2003. Functions evaluation of pedotransfer functions derived from different scales of data collection. Soil Sci. Soc. Am. J. 67, 1093–1102.
Nemes, A., Rawls, W.J., van Genuchten, M.J., 2006. Sensitivity analysis of the non parametric nearest neighbor technique to estimate soil water retention. Vadose Zone J. 5, 1222–1235.
Nemes, A., Roberts, R.T., Rawls, W.J., Pachepsky, Ya.A., van Genuchten, M.Th, 2008. Software to estimate – 33 and – 1500 kPa water retention using the non parametric k-nearest neighbor technique. Envir. Model. Softw. 23, 254–255.
Nguyen, P.M., De Pue, J., Le, K.V., Cornelis, W., 2015. Impact of regression methods on improved effects soil water retention estimates. J. Hydrol. 525, 598–606.
Pachepsky, Y.A., Rawls, W.J., 1999. Accuracy and reliability of pedotransfer functions as affected by grouping soils. Soil Sci. Soc. Am. J. 63, 1748–1757.
Pachepsky, Y.A., Timlin, D., Varallyay, G., 1996. Artificial neural networks to estimate soil water retention from easily measurable data. Soil Sci. Soc. Am. J. 60, 727–733.
Pachepsky, Y.A., Rawls, W.J., Lin, H.S., 2006. Hydropedology and pedotransfer functions. Geoderma 131, 308–316.
Patil, N.G., Singh, S.K., 2016. Pedotransfer functions for estimating soil hydraulic properties: a review. Pedosphere 26, 417–430.
Paydar, Z., Cresswell, H.P., 1996. Water retention in Australian soils. 2. Prediction using particle size, bulk density, and other properties. Aust. J. Soil Res 34, 679–693.
Petersen, G.W., Cunningham, R.L., Matelski, R.P., 1968. Moisture characteristics of Pennsylvania soils: I. Moisture retention as related to texture. Soil Sci. Soc. Am. J. 32, 271–275.
Piedallu, C., Gégout, J.C., Bruand, A., Seynave, I., 2011. Mapping soil water holding capacity over large areas to predict potential production of forest stands. Geoderma 160, 355–366.
Rawls, W.J., Brakensiek, D.L., Saxton, K.E., 1982. Estimation of soil water properties. Trans. ASAE 26, 1747–1752.
Rawls, W.J., Pachepsky, Y.A., Ritchie, J.C., Sobecki, T.M., Bloodworth, H., 2003. Effect of soil organic carbon on soil water retention. Geoderma 116, 61–76.
Rawls, W.J., Nemes, A., Pachepsky, Y.A., 2004. Effect of Soil Organic Carbon on Soil Hydraulic Properties, 30. Elsevier B.V., pp. 95–114.
Reeve, M.J., Smith, P.D., Thomasson, A.J., 1973. Effect of density on water retention properties of field soils. J. Soil Sci. 24, 355–367.
Reeve, M.J., Thomasson,A.J., Wright, V.F., 1977. Water retention, porosity and density of field soils. Soil Survey Technical Monograph N°9, Harpenden, 75p.
Reichert, J.M., Albuquerque, J.A., Solano Paraza, J.E., da Costa, A., 2020. Estimating water retention and availability in cultivated soils of southern Brazil. Geoderma Reg. 21, e00277.
Ribeiro, B.T., da Costa, A.M., Silva, B.M., Franco, F.O., Borges, C.S., 2018. Assessing pedotransfer functions to estimate the soil water retention. Biosci. J. 34, 177–188.
Richer-de-Forges, A.C., Arrouays, D., Chen, S., Román Dobarco, M., Libohova, Z., Roudier, P., Minasmy, B., Boureennane, H., 2022. Hand-feel soil texture and particle-size distribution in central France. Relationships and implications. Catena 213, 106155.
Ritchey, E.L., McGrath, J.M., Gehring, D., 2015. Determining Soil Texture by Feel. Agriculture and Natural Resources Publications. 139. University of Kentucky, College of Agriculture, Food and Environment, Lexington, KY, 40546, USA.
Robert, M., Tessier, D., 1974. Méthode de préparation des argiles des sols pour les études minéralogiques. Ann. Agron. 25, 859–882.
Rudiyanto, Minasny, B., Chaney, N.W., Maggi, F., Giap, S.G.E., Shah, R.M., Fiantis, D., Setiawan, B.I., 2021. Pedotransfer functions for estimating soil hydraulic properties from saturation to dryness. Geoderma 403, 115194.
Saby, N.P.A., Arrouays, D., Jolivet, C., Martin, M.P., Lacoste, M., Ciampalini, R., Deforges, A.C.R., Laroche, B., Bardy, M., 2014. National soil information and potential for delivering GlobalSoilMap products in France: A review. In: Globalsoilmap: basis of the global spatial soil information system, Proceedings of the 1st Conference on GlobalSoilMap (Ed. Arrouays, D., McKenzie N., Hempel J., Deforges A.C.R., McBratney A.), 69–72.
dos Santos, W.J.R., Curi, N., Silva, S.H.G., de Araújo, E.F., Marques, J.J., 2013. Pedotransfer functions for water retention in different soil classes from the centre-southern Rio Grande do Sul State. Ciência e Agrotechnologia 37, 49–60.
Schaap, M.G., Leij, F.J., 1998. Using neural networks to predict soil water retention and soil hydraulic conductivity. Soil Till. Res. 47, 37–42.
Schaap, M.G., Leij, F.J., van Genuchten, M.Th, 1998. Neural network analysis for hierarchical prediction of soil hydraulic properties. Soil Sci. Soc. Am. J. 62, 847–855.
Schaap, M.G., Leij, F.J., van Genuchten, M.Th, 2001. ROSETTA: a computer program for estimating soil hydraulic parameters with hierarchical pedotransfer functions. J. Hydrol. 251, 163–176.
Shaap, M.G., Bouten, W., 1996. Modelling water retention curves of sandy soils using neural networks. Water Resour. Res. 32, 3033–3040.
Singh, A., Haghverdi, A., Ozturk, H.S., Durner, W., 2020. Developing pseudo continuous pedotransfer functions for international soils measured with the evaporation method and the HYPROP system: I. The soil water retention curve. Water 12, 3425.
Skalova, J., Cisty, M., Bezak, J., 2011. Comparison of three regression models for determining water retention curves. J. Hydrol. Hydrom. 59, 275–284.
Stumpp, C.S., Engelhardt, M., Hofmann, M., Huwe, B., 2009. Evaluation of pedotransfer functions for estimating soil hydraulic properties of prevalent soils in a catchment of the Bavarian Alps. Eur. J. . Res 128, 609–620.
Thien, S.J., 1979. A flow diagram for teaching texture by feel analysis. J. Agron. Educ. 8 (1), 54–55.
Tian, Z., Chen, J., Cai, C., Gao, W., Ren, T., Heitman, J.L., Horton, R., 2021. New pedotransfer functions for soil water retention curves that better account for bulk density effects. Soil Till. Res. 205, 104812.
Twarakavi, N.K.C., Simunek, J., Schaap, M.G., 2009. Development of pedotransfer functions for estimation of soil hydraulic parameters using support vector machines. Soil Sci. Soc. Am. J. 73, 1443–1452.
Twarakavi, N.K.C., Sakai, S., Simunek, J., 2009. An objective analysis of the dynamic nature of field capacity. Water Resour. Res. 45, W10410.
Vapnik, V., 2013. The Nature of Statistical Learning Theory. Springer Science and Business Media, New York.
Veihmeyer, F.J., Hendrickson, A.H., 1927. The relation of soil moisture to cultivation and plant growth. Proc.1th intern. Congr. Soil Sci. 3, 498–513.
Vereecken, H., Maes, J., Feyen, J., Darius, P., 1989. Estimating the soil moisture retention characteristics from texture, bulk density and carbon content. Soil Sci. 148, 389–403.
Vereecken, H., Weynants, M., Javaux, M., Pachepsky, Y., Schaap, M.G., van Genuchten, M.Th, 2010. Using pedotransfer functions to estimate the van Genuchten-Mualem soil hydraulic properties: a review. Vadose Zone J. 9, 795–820.
Williams, J., Prebble, R.E., Williams, W.T., Hignett, C.T., 1983. The influence of texture, structure and clay mineralogy on the soil moisture characteristics. Aust. J. Soil Res. 21, 15–32.
Wösten, J.H.M., Lilly, A., Nemes, A., Le Bas, C., 1999. Development and use of a database of hydraulic properties of European soils. Geoderma 90, 169–185.
Wösten, J.H.M., Pachepsky, Y.A., Rawls, W.J., 2001. Pedotransfer functions: bridging the gap between available basic soil data and missing soil hydraulic characteristics. J. Hydrol. 251, 123–150.
Zhang, Y.G., Schaap, M.G., Wei, Z.W., 2020. Development of hierarchical ensemble model and estimates of soil water retention with global coverage. Geophys. Res. Lett. 47. . e2020GL088819.